Catalysis Today 145 (2009) 19–26

Contents lists available at ScienceDirect

Catalysis Today

journal homepage: www.elsevier.com/locate/cattod

Lithium ions incorporation in MgO for oxidative dehydrogenation/cracking of propane: Active site characterization and mechanism of regeneration

C. Trionfetti, S. Crapanzano, I.V. Babich, K. Seshan [*], L. Lefferts

Catalytic Processes and Materials Group, Faculty of Science and Technology, IMPACT, University of Twente, Enschede, The Netherlands

ARTICLE INFO

Article history:
Available online 15 August 2008

Keywords:
Oxidative dehydrogenation/cracking of propane
Li-promoted MgO
Active site regeneration
De-hydroxylation reaction

ABSTRACT

In the case of Li-promoted MgO two different mechanisms for regeneration of the active site are found when varying the temperature between 550 and 700 °C. Propane titration showed that the active site is deactivated through formation of hydroxyl groups that are stable at 550 °C and below in absence of oxygen. On the contrary at 700 °C, propane pulses resulted in hydrocarbon activation, accompanied by evolution of water molecules. In addition, simultaneous evolution of hydrogen molecules pulsing propane indicate that ODH of propane follows a mixed heterogeneous–homogeneous radical chemistry. No CO_x was observed while pulsing propane at both temperatures. Moreover CO_x molecules were not detected even during catalyst regeneration by pulsing oxygen showing that Li/MgO materials are not affected by coke formation. Formation of CO_x molecules seems to be feasible exclusively by co-feeding propane and oxygen.

1. Introduction

Traditionally, olefins are produced by non-catalytic conversion of hydrocarbons, i.e. steam cracking, which is industrially well proven but characterized by severe conditions and homogeneous phase radical chemistry that maximizes ethylene selectivity instead of propylene [1–3].

However, commercially available catalytic routes for olefins production, *viz.* catalytic dehydrogenation, also present several drawbacks because of thermodynamic equilibrium constraints and coking that restricts catalyst stability [4]. In this respect, oxidative dehydrogenation reactions (ODH) are considered as the most promising way to avoid thermodynamic limitations, minimize coking and limit the necessity of external heating during the production of olefins from light alkanes [5]. Indeed, when an oxidant, e.g., molecular oxygen, is added to the feed gas the process becomes thermodynamically favorable because of water formation.

In the case of ODH of propane, mainly two types of catalytic materials are discussed which differ in the nature and properties of surface-oxygen species taking part in the hydrocarbon activation. The first type of materials, classified as redox type catalysts, is mainly based on vanadium oxides as main component [6]. For these catalysts lattice oxygen is available for the catalytic cycle and considered to be responsible for the selective and non-selective reaction pathways leading to olefins, CO_x and water [7]. The second class of materials, i.e., non-redox type of catalysts, is based on MgO doped with alkali [8,9]. For these materials lattice oxygen cannot be consumed and replenished during the catalytic cycle [10]. As reported often in the case of methane coupling, the catalytic activity of Li-promoted MgO is determined by surface $[O^-]$ species and their existence in MgO was mainly shown using the electron paramagnetic resonance (EPR) technique [11–13]. Lunsford suggested that the $[O^-]$ species was created by the substitution of Li^+ for Mg^{2+} ions to allow charge balance and stabilized on the MgO lattice as $[Li^+O^-]$ centers [14]. Remarkably, $[O^-]$ are reported to be very stable at high temperatures and can exist in the crystal lattice of metal oxides even in the absence of oxygen in the gas phase [15].

It is experimentally proved, in the case of Li/MgO catalysts, that the first step in oxidative conversion of methane involves the homolytic scission of C–H bonds forming surface –OH groups and alkyl radicals (Eq. (1)) [16]:

$$[O^-]_{(s)} + CH_4 \rightarrow [OH^-]_{(s)} + CH_3^{\bullet} \quad (1)$$

The resulting radicals are released from the catalyst surface and subsequently initiate gas phase-chain propagation reactions to yield products [17].

---

[*] Corresponding author at: Catalytic Processes and Materials Group, Faculty of Science and Technology, IMPACT, University of Twente, Post Box 217, 7500 AE Enschede, The Netherlands. Tel.: +31 53 489 3254; fax: +31 53 489 4683.
E-mail address: k.seshan@utwente.nl (K. Seshan).

0920-5861/$ – see front matter © 2008 Elsevier B.V. All rights reserved.
doi:10.1016/j.cattod.2008.06.018

Assuming the proposed surface initiation as a primary step, Leveles et al. recently suggested a reaction mechanism to describe the oxidative conversion of propane over Li/MgO catalysts. Indeed, the mechanism involves a sequence in which the $[Li^{+}O^{-}]$ active site abstracts a hydrogen from propane forming *n*- or *iso*-propyl radicals that undergo radical chain reactions in the gas phase [8,9].

However, several uncertainties still exit concerning the way how the catalytic sequence is closed *via* the regeneration of the active site. One of the difficulties is to identify the mechanism how the hydrogen is removed from the surface $[OH^{-}]$ group. Ito and Lunsford suggested regeneration of surface hydroxyl groups to occur *via* de-hydroxylation reaction and hence removal of lattice oxygen that leaves an anion vacancy (Eq. (2)) [18,19]:

$$2[OH^{-}]_{(s)} \rightarrow [O^{2-}]_{(s)} + [V_a] + H_2O \quad (2)$$

Oxygen removal implies redox changes in the material, however, if this is the case for Li/MgO material is not established. In fact, water formation during ODH experiment is generally not easily detected and quantified even when using on-line gas chromatography. This becomes even more difficult when the catalysts are prepared using high temperature treatments ($T \geq 700$ °C) and thus possess low surface areas that result in low concentration of surface $[Li^{+}O^{-}]$ centers and hence low catalytic activity.

In one of our previous papers [20], we compared the surface properties and catalytic performance of Li/MgO catalysts prepared using wet impregnation procedures (imp) and sol–gel (sg) technique resulting, respectively, in low and high surface area materials. We reported, based on spectroscopic studies, that Li/MgO-sg catalysts show an enhanced concentration of incorporated Li^{+} ions. Interestingly, these tend to be localized in the MgO surface that also presents an enhanced concentration of defects which might also affect catalytic activity. In agreement with this observation/hypothesis, Li/MgO-sg catalysts showed higher catalytic activity for the oxidative propane conversion.

The aim of this paper is to quantify the number of active centers responsible for the catalytic activation of propane in Li^{+}-promoted MgO catalysts, prepared using wet impregnation and sol–gel technique. This might help to describe, respectively, (i) the role of Li^{+} incorporation in MgO in creating the active sites, and (ii) the properties of surface $[O^{-}]$ species stabilized as $[Li^{+}O^{-}]$ centers. In particular, we will attempt to investigate this by following possible reduction and re-oxidation processes. In the end we aim to establish the elementary reaction steps taking place on the catalyst surface during the active sites regeneration.

2. Experimental

2.1. Materials

Commercially available $Mg(OCH_3)_2$ solution (Aldrich, 8.7 wt.%, in methanol), methanol (Merck, GR for analysis), $LiNO_3$ (Merck, >99.0%) and MgO (Merck, 99.9%) were used. Water added to the solution was double de-ionized.

2.2. Catalyst preparation

A solution of $Mg(OCH_3)_2$ in methanol (0.4 M) containing $LiNO_3$ (in appropriate amounts to obtain 1, 3 and 5 wt.% Li in MgO) was mixed with water in methanol (0.8 M) at room temperature and allowed to stand for 24 h for gelation (wet gels). After drying at 50 °C in vacuum for 7 h the dried gels were calcined at 600 and 700 °C in air according to the method described in detail in [21]. These catalysts will be, hereafter, referred to as Li/MgO-sg. In addition, Li/MgO catalysts containing varying amounts of Li (1 and 5 wt.%) were also prepared using $LiNO_3$ *via* wet impregnation of MgO, hereafter referred to as Li/MgO-imp, according to the method described in detail in [21]. The impregnation step was followed by drying and calcination at 700 °C [9].

2.3. Catalyst characterization

Catalyst composition and the total concentration of impurities in the samples were measured by chemical analysis (AAS) and XRF (Philips PW1480). In addition to MgO the following were detected (maximum amount of wt.% shown in parentheses): Cs_2O (0.0002), SiO_2 (0.1), BaO (0.002), CaO (0.03), K_2O (0.002) and S (0.04).

Presence of different lithium phases as well as the amount of lithium incorporated in MgO was valuated by X-ray diffraction [22]. Patterns were recorded with a Philips PW 1830 diffractometer using Cu Kα radiation, λ = 0.15418 nm. Catalysts compositions and the amount of incorporated lithium in MgO are presented in Table 1. Surface area was measured with N_2 adsorption measurements and experiments were carried out using a Micrometrics Tristar instrument. The samples were out gassed in vacuum at 200 °C for 24 h prior the analysis.

2.4. Pulse experiments

Reduction–oxidation cycles were carried out in a quartz reactor (internal diameter 4 mm) under plug flow conditions at atmospheric pressure. The catalyst bed was packed between two quartz-wool plugs. Approximately 100 mg of catalyst was used. In all experiments the catalyst was activated in 10% O_2 in He for 1 h at temperatures 50 °C higher than that desired for the experiments (550 and 700 °C). The reduction was performed by treating the catalysts in 10% H_2 in He at 550 °C for 1 h. After purging the sample in He for 30 min, pulses of 2% O_2 in He flow as carrier (loop volume 500 μl) were sent through the catalytic bed. The outlet of the reactor was directly connected to a gas chromatography (GC). The pulses were sent *via* a Porapak column to a thermal conductivity detector (TCD) to observe and quantify the consumption of oxygen.

Propane and hydrogen titration tests were also carried out in a kinetic setup employing a quartz fixed bed reactor. Quartz beads were inserted upstream and downstream of the catalyst bed to minimize the empty volume. After activation (10% O_2 in He) the system was purged in He flow (total flow rate 3 ml/min) until a constant level of oxygen (zero level) was recorded. Each pulse (loop size 300 μl) containing only one reactant, i.e., propane, hydrogen and oxygen diluted in He (95%) was sent separately to the catalyst bed. The feed and the effluent compositions were monitored by sampling on-line to a quadrupole mass analyzer (Pfeiffer AG Balzers, OmniStar) equipped with Channeltron and Faraday detectors (2–200 amu).

Table 1
Chemical composition and surface area of the Li/MgO catalyst prepared, respectively, using sol–gel method (sg) and wet impregnation (imp)

Sample	Total lithium (wt.%)	Lithium incorporated (wt.%)[a]	BET (m^2/g)
MgO-sg	0	0	60
1 wt.% Li/MgO-sg	1	0.5	50
3 wt.% Li/MgO-sg	3	0.7	30
5 wt.% Li/MgO-sg	5	0.9	25
MgO (Merck)	0	0	30
1 wt.% Li/MgO-imp	1	0.1	9
5 wt.% Li/MgO-imp	5	0.5	4

[a] Amount of lithium incorporated in MgO was estimated by XRD, for details see [22].

2.5. Carbon dioxide sorption experiments

Sorption measurements were used to investigate the interaction of CO_2 on the surface of pure MgO and Li-promoted MgO catalysts. Experiments were carried out with a Mettler-Toledo TGA-SDTA apparatus at temperatures between 100 and 700 °C. Typically 40–80 mg of sample was used in a 70 μl alumina crucible. A gas flow of 50 ml/min with a composition of 10% CO_2 in Argon was used. Prior the experiments the samples were pretreated at 700 °C in Argon until a constant weight was measured.

3. Results

3.1. Properties of the catalysts tested

Table 1 shows the list of all the catalysts tested. The catalyst surface area and the relative amount of incorporated Li in MgO (estimated by XRD) are also shown. Li/MgO-sg catalysts possess, respectively, higher surface areas and amounts of lithium built into MgO lattice than Li/MgO-imp catalysts (Table 1). In fact, as we reported in our earlier contributions about catalyst preparation [21], during the sol–gel method lithium ions can be incorporated in the magnesia gel structure and high temperatures treatments are not required.

3.2. Li/MgO active sites titration: reduction/oxidation cycles and CO_2 sorption

In previous papers, Leveles et al. proposed that the formation of $[Li^+CO_3^-]$ species by CO_2 interaction with the $[Li^+O^-]$ active site can be observed and quantified [9]. This would make CO_2 a suitable probe molecule in order to titrate and quantify the number of catalytically active $[O^-]$ species. Thus, the interaction of CO_2 molecules with the Li/MgO catalysts was studied using TGA. Fig. 1 shows a typical experimental result during the sorption/desorption cycles of CO_2 at temperatures between 100 and 700 °C over 1 wt.% Li/MgO-sg catalysts. The experiments were carried out under conditions where the desorbed CO_2 molecules from $[Li^+CO_3^-]$ surface specie may be differentiated from those attributed to the decomposition of Li_2CO_3. Switching on CO_2 containing inert gas (Ar) to the sample in TGA results in a weight increase for all the tested temperatures (Fig. 1, left-hand). Adsorption of CO_2 reached steady state after 20 min at 700 °C. Switching off CO_2 from the gas stream did not cause any changing in weight at low temperature i.e., 100 °C while at temperature higher than 500 °C it resulted in a weight decrease of the sample due to CO_2 partially desorbed (Fig. 1, right-hand). In particular, at temperature of 700 °C, CO_2 desorption did not reach steady state during the measurements. On the contrary, desorption at 550 °C quickly reached the equilibrium already after 10 min.

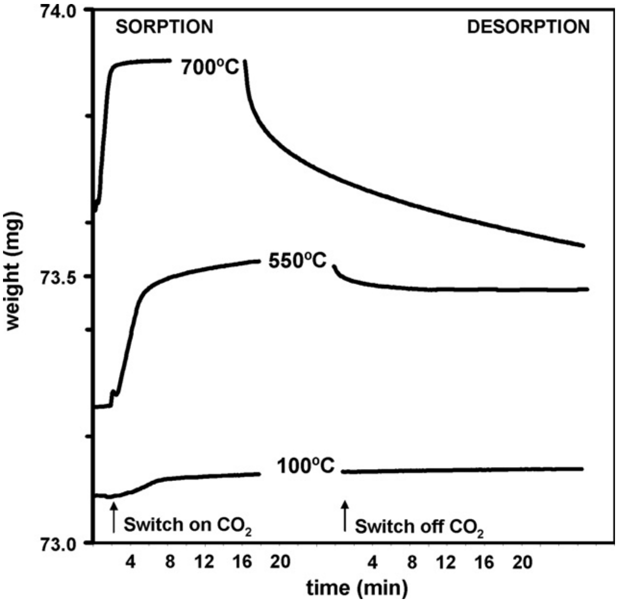

Fig. 1. Sorption and desorption curves measured in TGA on 1 wt.% Li/MgO sol–gel catalyst. Conditions: 10% CO_2 in Ar; total flow 50 ml/min.

The adsorption/desorption cycles were performed at 550 °C in TGA for all the catalysts prepared using sol–gel method and wet impregnation (samples containing varying amounts of lithium) and the results are reported in Table 2.

The first column shows the number of moles of CO_2 desorbed at 550 °C expressed per m^2 of catalyst. Appreciably, for both Li/MgO-sg and Li/MgO-imp catalysts the concentration of CO_2 desorbed increased with increasing lithium content. Interestingly, we observed that the amounts of CO_2 desorbed per m^2 of catalyst for Li/MgO-sg samples were in the same range as obtained for Li/MgO-imp catalysts (Table 2). We can conclude from this that the surface area of Li/MgO catalysts can be tuned without altering nature and properties of the materials (see Tables 1 and 2).

The second method to quantify the number of surface $[Li^+O^-]$ active sites consists of measuring the amount of oxygen consumed while pulsing O_2 containing stream over catalysts (pretreated in hydrogen at $T = 550$ °C followed by purging with He). The typical result of this experiment is presented in Fig. 2 for 1 wt.% Li/MgO-sg catalyst. The oxygen TCD signal shows that the catalyst treated in hydrogen consumed all the oxygen molecules from the first pulse and nearly half of the second pulse ($\sim 10^{-6}$ moles of oxygen atoms). An investigation of the reaction taking place during reduction and oxidation processes over Li/MgO catalysts will be shown in the next paragraph and discussed afterwards. Quantitative data (using TCD) for oxygen consumption during pulsing at 550 °C for all the

Table 2
Results of oxygen titration obtained from reduction/oxidation cycles (columns 2–4) for MgO and Li/MgO catalysts prepared using sol–gel method (sg) and wet impregnation (imp)

Sample	Moles of CO_2 desorbed per m^2 of catalyst ($\times 10^{-7}$)	Amount of O_T as % of total available oxygen	Amount of O_T as % of surface available oxygen	Moles of O_T per m^2 of catalyst ($\times 10^{-7}$)
MgO-sg	0.08	0.01	0.3	0.4
1 wt.% Li/MgO-sg	2.7	0.04	1.5	2.1
3 wt.% Li/MgO-sg	4.9	0.04	2.7	3.5
5 wt.% Li/MgO-sg	7.5	0.06	4.5	5.9
MgO	0.003	0.005	0.3	0.4
1 wt.% Li/MgO-imp	2.0	0.008	1.6	2.0
5 wt.% Li/MgO-imp	6.9	0.011	4.6	6.0

The amount of CO_2 desorbed per m^2 of catalyst (column 1) is also shown. All the experiments were carried out at $T = 550$ °C.

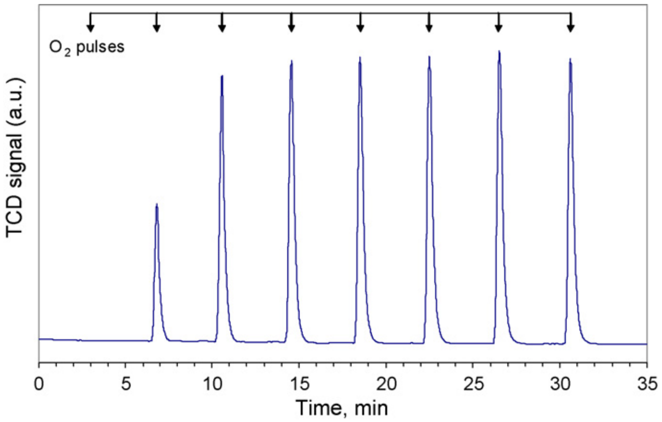

Fig. 2. TCD signal during oxygen pulsing of pretreated 1 wt.% Li/MgO catalyst prepared using sol–gel method. Pretreatment: 10% hydrogen, 1 h at 550 °C. Carrier (He) flow: 30 ml/min.

catalysts prepared using sol–gel method and wet impregnation are shown in Table 2.

The column 2 in Table 2 shows the amount of titrated oxygen atoms (O_T) expressed as percentage of the total number of oxygen present in the sample. Furthermore, in columns 3 and 4 the amount of O_T is calculated as, respectively, (i) percentage of total surface oxygen atoms and (ii) moles of oxygen atoms per m^2 of catalyst. These two were calculated taking in consideration the surface area of each catalyst and assuming the face (0 0 1) of MgO as the only one exposed (surface oxygen density of 0.45 oxygen atoms/Å^2 considering, respectively, (i) a cube with 4 MgO, and (ii) the Mg–O bond distance similar to 2.1 Å).

In summary, Table 2 shows that for both Li/MgO-sg and Li/MgO-imp catalysts the number of titrated surface oxygen species increased with increasing lithium content (column 2). Moreover, the number of moles of titrated oxygen atoms normalized per m^2 of catalysts is the same (column 4). The results from adsorption/desorption of CO_2 and reduction/oxidation cycles show a good correlation (column 1 and 4). However, an appreciable difference was observed only in the case of MgO. In this case, the number of moles of [O^-] specie (normalized per m^2) estimated using CO_2 sorption is much lower than the one calculated from the re-oxidation experiments.

3.3. Regeneration of the active site: hydrogen and propane pulses at 550 °C

A typical experimental result during subsequent pulsing of H_2 and O_2 over 5 wt.% Li/MgO-sg catalyst at 550 °C is presented in Fig. 3. Prior to the experiments all the catalysts were treated in 10% oxygen in He at 600 °C for 1 h and then purged in He flow for 30 min to remove any oxygen molecules physisorbed on the surface. Results in Fig. 3 show that hydrogen pulses resulted in partial consumption of hydrogen without formation of any product water. Moreover, after two pulses (out of five) no appreciable consumption of hydrogen was recorded (surface deactivation). After purging in He for a few minutes (to remove adsorbed hydrogen) subsequent O_2 pulses were sent through the catalytic bed. Consumption of oxygen and formation of H_2O were simultaneously observed (surface regeneration, Fig. 3). Catalyst re-oxidation seemed to be facile since most of hydrogen was removed after the first O_2 pulse. Second set of H_2 and O_2 pulses produced the same results, respectively, H_2 consumption without H_2O production and simultaneous O_2 consumption and H_2O production. The mechanism of this re-oxidation will be discussed later in the manuscript.

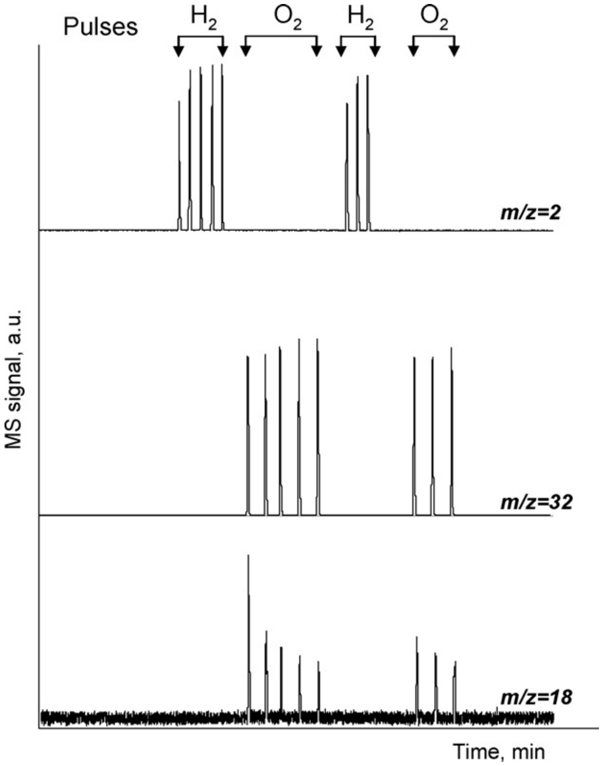

Fig. 3. MS signal intensity during hydrogen and oxygen pulsing at 550 °C of pretreated Li/MgO sol–gel catalyst; pretreatment in 10% oxygen in He, 1h at 600 °C and then purged 30 min in pure He.

We shall now discuss the results obtained in the case of subsequent pulses of propane and oxygen. In Fig. 4 a typical experimental result over 5 wt.% Li/MgO-sg catalyst is shown. During propane pulses consumption of propane was observed which can be attributed to the activation of propane on the catalyst surface. In addition, formation of hydrogen was simultaneously detected (Fig. 4). In particular, the MS signal intensity of H_2 quickly drops down after the first propane pulse (fast surface deactivation). Interestingly, this contribution can be attributed to reactions taking place in the gas phase and discussed later. After purging the sample in He pulses of O_2 were sent through the catalytic bed. As it was previously observed (Fig. 3), simultaneous oxygen consumption and formation of water was recorded (Fig. 4). Remarkably, formation of CO_x was not detected during pulsing $C_3{}^0$ and even during pulsing of O_2 (results not shown here). Thus, the catalysts do not seem to suffer from coke formation. To summarize, all the observations here reported suggest that formation of water in the catalytic cycle occurs exclusively with gas phase oxygen.

3.4. Regeneration of the active site: hydrogen and propane pulses at 700 °C

Experimental results during subsequent pulses of H_2 and O_2 at 700 °C over 5 wt.% Li/MgO-sg catalyst are shown in Fig. 5 In contrast to the results showed in Fig. 3 during repetitive H_2 pulses, consumption of hydrogen was accompanied by the evolution of molecules of water (Fig. 5). Remarkably, formation of water involves necessarily the partial removal of oxygen atoms from the lattice of Li/MgO catalysts and additionally formation of oxygen vacancies (Eq. (2)). Surprisingly, at 700 °C Li/MgO catalysts show appreciable hydrogen consumption. After purging the samples in He, consecutive oxygen pulses were performed and showed exclusively

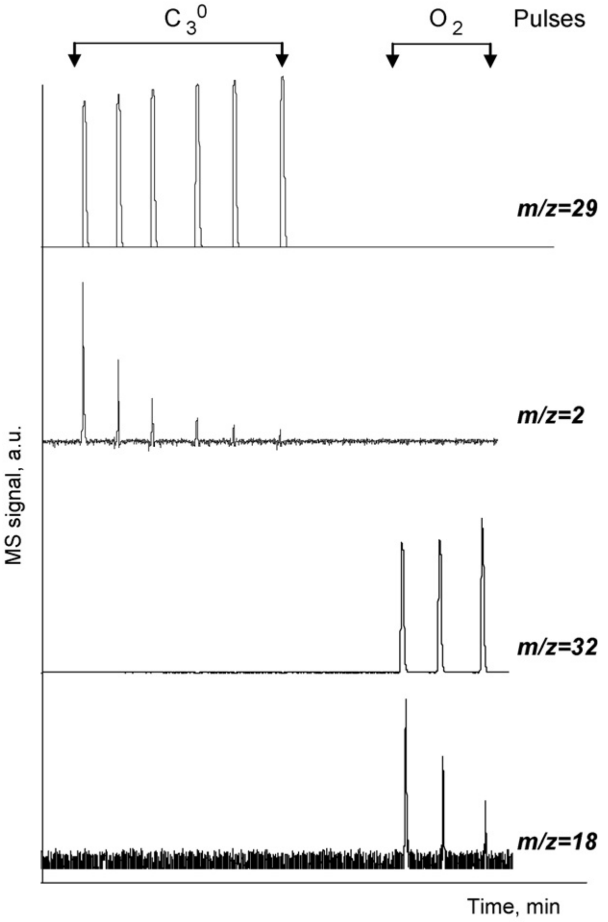

Fig. 4. MS signal intensity during propane and oxygen pulsing at 550 °C of pretreated Li/MgO sol–gel catalyst; pretreatment in 10% oxygen in He, 1 h at 550 °C and then purged 30 min in pure He.

consumption of oxygen. In fact, not even a trace of water formation was detected (Fig. 5).

The results of subsequent pulses of propane and oxygen at 700 °C over 5 wt.% Li/MgO sol–gel catalyst are presented in Fig. 6. In particular, during pulses of propane, (i) consumption of propane, (ii) evolution of hydrogen, and (iii) formation of water molecules were simultaneously observed (Fig. 6).

Remarkably, in contrast to the results obtained at 550 °C (Fig. 4) formation of H_2O showed the removal of oxygen atoms from the catalyst lattice structure during pulses of propane (Eq. (2)). Surprisingly, formation of CO and CO_2 molecules was not recorded. In the case of CO, a quantitative detection was less spectacular at 700 °C and CO traces cannot be excluded completely. This is due to the large presence of products having fragmentation pattern similar to carbon monoxide, $m/z = 28$ (i.e., propylene and ethylene) [23]. As expected, pulses of oxygen showed clearly consumption of oxygen but no traces of water formation (Fig. 6). Moreover, CO and CO_2 were also not detected suggesting again that the catalyst is not affected by coke formation.

4. Discussion

It is a general knowledge that the conversion of light alkanes (C_1–C_4 range) on Li-promoted MgO proceeds *via* a heterogeneous–homogeneous mechanism, in which alkyl radicals are generated on the catalyst surface and released to the gas phase [24,25]. In the case of oxidative conversion of propane, Leveles et al. [9] demonstrated the crucial role of lithium in creating an active catalytic site. Moreover, Ito et al. showed that Li^+ ions occupying Mg^{2+} sites can stabilize the nearby $[O^-]$ species resulting in $[Li^+O^-]$ defects sites [18]. Thus, propyl radicals can be formed *via* homolytic hydrogen abstraction on $[Li^+O^-]$ centers to form surface hydroxyl groups $[OH^-$. Subsequently, these sites may be regenerated with the help of gas phase oxygen molecules [26].

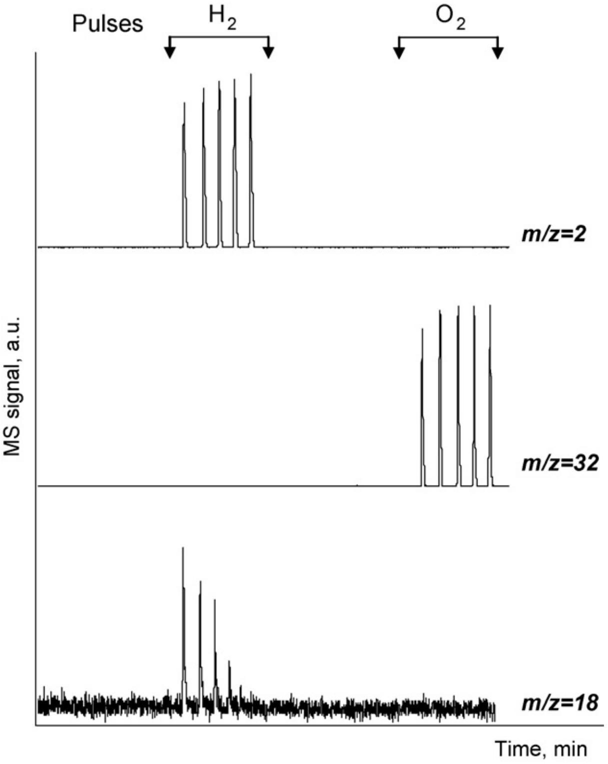

Fig. 5. MS signal intensity during hydrogen and oxygen pulsing at 700 °C of pretreated Li/MgO sol–gel catalyst; pretreatment in 10% oxygen in He, 1 h at 700 °C and then purged 30 min in pure He.

We shall first discuss our attempts to quantify the number of surface $[Li^+O^-]$ active sites. Furthermore, the mechanism of regeneration of the active site will be clarified. Presence of $[O^-]$ ions on several metal oxides has been proposed and based only on electron magnetic resonance technique (ESR). In this respect, the only reactions studied on the surface of such metal oxide systems are those in which stable paramagnetic radicals are formed. Examples of these reactions are [27,28]:

$$O^- + O_2 \rightarrow O_3^- \tag{3}$$

$$O^- + CO_2 \rightarrow CO_3^- \tag{4}$$

In addition, CO_2 molecule adsorbed on $[Li^+O^-]$ was detected by *in situ* IR spectroscopy and it was concluded that $[Li^+CO_3^-]$ species is the precursor for Li_2CO_3 formation [29]. Thus, CO_2 can poison, reversibly, the active sites. But at the same time CO_2 also stabilizes the catalyst against deactivation in oxidative coupling at relatively high temperature [30] by forming carbonates species, preventing the formation of volatile Li(OH) compounds [31].

Based on previous studies from Leveles et al. [9] the number of $[Li^+O^-]$ active sites can be quantified using CO_2 as probe molecule and involving its reversible adsorption/desorption reaction on the $[Li^+O^-]$ sites. In particular, the following assumptions were made: (i) CO_2 molecules are reversibly adsorbed on the Li/MgO surface exclusively forming $[Li^+CO_3^-]$, and (ii) the number of moles of desorbed CO_2 molecules is equal to the number of moles of active

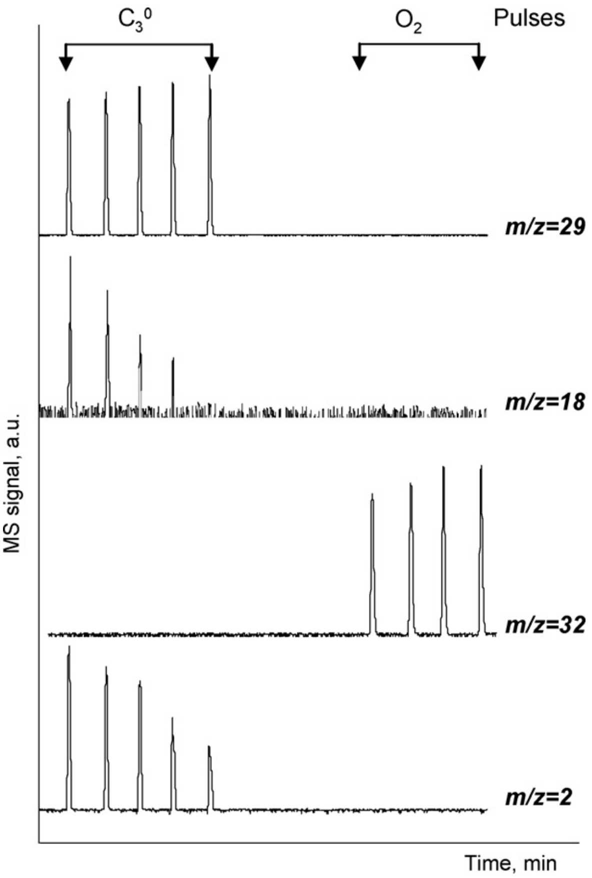

Fig. 6. MS signal intensity during propane and oxygen pulsing at 700 °C of pretreated Li/MgO sol–gel catalyst; pretreatment in 10% oxygen in He, 1 h at 700 °C and then purged 30 min in pure He.

$[O^-]$ species. Fig. 1 shows two distinct modes of CO_2 adsorption. At relative low temperature i.e., 100 °C the adsorption is irreversible. The adsorbed CO_2 molecules give rise to the formation of $MgCO_3$ and Li_2CO_3 and switching off CO_2 from the stream does not result in any desorption of carbon dioxide. On the contrary, at $T \geq 550$ °C the adsorption is, at least partly, reversible. In particular, at the temperature of 550 °C a fast but incomplete CO_2 desorption is recorded (Fig. 1). It is here appropriate to stress that 550 °C is higher than the temperature of $MgCO_3$ decomposition (450 °C) [32] and lower than Li_2CO_3 decomposition (700 °C) [32]. Therefore, at $T = 550$ °C MgO would not show any sorption of CO_2 and this contribution can be ruled out (see Table 2). Thus, the desorption phenomena at 550 °C can be associated to the release of CO_2 from unstable $[Li^+CO_3{}^-]^-$ species (Eq. (5)):

$$[Li^+O^-] + CO_2 \Leftrightarrow [Li^+CO_3{}^-] \quad (5)$$

Non-removed CO_2 should be related to formation of Li_2CO_3 which is stable at this temperature. Moreover, complete desorption of CO_2 is recorded at temperatures above 700 °C due to the contribution of Li_2CO_3 decomposition (Fig. 1). In summary, considering the number of moles of CO_2 desorbed at 550 °C equal to the number of moles of surface $[O^-]$ species we found that the concentration of $[Li^+O^-]$ active sites increases with increasing lithium content, Table 2 (for both Li/MgO-sg and Li/MgO-imp samples).

Let us now discuss the results obtained from treating the catalyst in hydrogen and then pulsing oxygen through the catalytic bed. Interestingly, Leveles et al. observed that at 600 °C the samples pretreated in hydrogen markedly lose their reactivity in propane oxidative dehydrogenation [9]. This fact can be explained by deactivation of surface active sites which are involved in oxidation of propane. Interestingly, they proposed that the catalytic activity of Li/MgO catalysts can be attributed to removable lattice oxygen. Thus, they suggested that active $[O^-]$ species possess peculiar properties and these can be removed during hydrogen treatment at high temperatures and replenished exclusively upon oxygen treatment [9]. However, this would imply the formation/evolution of species containing oxygen i.e., H_2O during hydrogen treatment but no direct observation of that was reported [9].

Similarly, the results presented in Fig. 2 show appreciable consumption of oxygen during oxygen pulses preformed at 550 °C over samples pretreated in hydrogen. At this stage, we attribute the estimated oxygen consumption to the removal of hydrogen adsorbed on the catalyst surface. In particular, we calculated the number of $[Li^+O^-]$ active sites assuming that, respectively, (i) adsorbed H_2 molecules can be split homolitically on surface active $[O^-]$ species forming hydroxyl groups (Eq. (6)) and (ii) each $[O^-]$ specie belongs to the $[Li^+O^-]$ active site.

$$H_2 + 2O^- \rightarrow 2[OH^-] \quad (6)$$

Interestingly, for both Li/MgO-sg and Li/MgO-imp catalysts oxygen consumption increases with increasing lithium content (Table 2) reflecting the increased number of active sites. Interestingly, the concentration of active sites estimated from desorbed CO_2 and oxygen consumption is in the same range (Table 2). To summarize, in the explored range of lithium doping, Li/MgO-sg samples having higher surface area than Li/MgO-imp materials posses the same number of active sites per m^2 of catalyst (Table 2).

It is now appropriate to discuss the mechanism of active site regeneration for Li/MgO catalysts. To our knowledge, the only complete mechanism for the oxidative conversion of alkane (i.e., CH_4) over Li-promoted MgO, including activation and regeneration of the active site, was proposed by Ito and Lunsford [18,19]. For the present case, as discussed above, let us speculate that the oxidative dehydrogenation/cracking of propane proceeds along the same mechanism. Similar to Eq. (1) the first step includes hydrogen abstraction by $[Li^+O^-]$ defects with formation of two surface $[OH^-]$ groups:

$$2[Li^+O^-] + 2C_3H_8 \rightarrow 2[Li^+OH^-] + 2C_3H_7{}^\bullet \quad (7)$$

The formed propyl radicals are released to the gas phase where they undergo radical chain reactions. The second step, according to Eq. (2), involves dissociation of one surface $[OH^-]$ group into a lattice O^{2-} ion and a mobile surface proton. This proton migrates to another $[OH^-]$ group to form a water molecule which desorbs from the surface leaving behind an anion vacancy (V_a):

$$2[Li^+OH^-] \rightarrow [Li^+O^{2-}] + [Li^+V_a] + H_2O \quad (8)$$

The final step [18,19] is the regeneration of the active site, which involves electron transfer to the anion vacancy and the dissociative chemisorption of oxygen, respectively, Eqs. (9) and (10):

$$[Li^+O^{2-}] + [Li^+V_a] \rightarrow [Li^+O^-] + [Li^+V_a{}^-] \quad (9)$$

$$[Li^+V_a{}^-] + O_2 \rightarrow [Li^+O^-] + O \quad (10)$$

However, certain features in the Ito–Lunsford mechanism appear to be unlikely especially at lower temperatures. In particular, removal of oxygen from the lattice is not facile and this would be the rate-limiting step of the complete catalytic cycle (instead of hydrogen abstraction) [18]. Moreover, migration of a proton, as in reaction (8) would require, respectively, (i) substantial energy to overcome electrostatic barrier [33], and (ii) the proximity of $[Li^+O^-]$ centers [34].

Alternatively, Sinev et al. [35] and Sinev [36] proposed a new mechanism of regeneration of the active sites that does not require the removal of lattice oxygen and thus the formation of oxygen vacancies. In fact, the re-oxidation of the catalyst can proceed by the mechanism of oxidative dehydrogenation of surface OH groups and require the scission of strong O–H bonds. More specifically, regeneration reactions proposed by Sinev are summarized here [37]:

$$O_2 + [OH^-] \rightarrow [O^-] + HO_2^{\bullet} \quad (11)$$

$$HO_2^{\bullet} + [OH^-] \rightarrow [O^-] + H_2O_2 \quad (12)$$

$$H_2O_2 \rightarrow 2^{\bullet}OH \quad (13)$$

$$^{\bullet}OH + [OH^-] \rightarrow [O^-] + H_2O \quad (14)$$

It is appropriate to stress that the overall equation of regeneration is the same as in the mechanism proposed by Ito and Lunsford [18]. In fact, it involves the participation of two surface $[OH^-]$ groups and the formation of water molecules. However, it does not require removal of lattice oxygen. As we mentioned above, for both Li/MgO-sg and Li/MgO-imp catalysts during pulses of propane and hydrogen at 550 °C initial conversion of reactants and catalyst deactivation was observed (Figs. 3 and 4). Additionally, the deactivation was not accompanied by water formation. This implies surface deactivation without any lattice oxygen removal and, most likely, formation of oxygen vacancies as intermediate stage does not take place. To conclude, under these conditions surface $[OH^-]$ groups are formed and result to be stable in absence of gas phase oxygen. Thus, Li/MgO catalysts do not show any reducibility at 550 °C.

Remarkably, only during the interaction of oxygen with the catalysts pretreated in propane or hydrogen the evolution of water was observed. This may suggest, as proposed by Sinev, that at 550 °C the re-oxidation of Li/MgO catalysts proceeds as some sort of oxidative dehydrogenation of surface hydroxyl groups (Scheme 1 and Eqs. (11)–(14)). Our observations suggest that only at higher temperatures (700 °C) and relevant to methane coupling discussed by Lunsford, the catalyst regeneration goes *via* the traditional scheme of re-oxidation, according to Ito and Lunsford mechanism that implies a de-hydroxylation step involving the formation of oxygen vacancies.

Finally we would like to discuss the formation of hydrogen observed during pulses of propane. Typically, homolytic C–H bond splitting forming propyl radicals is the rate determining step [38]. For the propyl radicals formed, mainly two different decompositions routes have been proposed in gas phase in absence of oxygen. In general, there is a slight preference for, (i) C–H bond scission at the α-position to yield propylene and H radical and (ii) C–C cleavage in the β-position forming methyl radical and ethylene [8]. However, a series of gas phase reactions involving propyl radicals that lead to the formation of H_2 molecules are suggested in literature and here reported [8,39].

$$i\text{-}C_3H_7^{\bullet} \rightarrow C_3H_6 + H^{\bullet} \quad (15)$$

$$H^{\bullet} + C_3H_8 \rightarrow H_2 + C_3H_7^{\bullet} \quad (16)$$

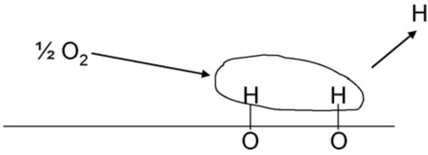

Scheme 1. Schematic drawing: mechanism of regeneration of the active sites as suggested by Sinev et al. [35].

This argument can be logically connected to the amounts of hydrogen that we observed during pulses of propane. In fact, our observations suggest that catalytic formation of alkyl radical and homogeneous gas phase radical reactions take place even during pulse experiments. Furthermore, comparison between the MS signal intensities of hydrogen formed during propane pulses at 550 °C and 700 °C (see Figs. 4 and 6) supports the role for homogeneous gas phase reactions which are favored at higher temperatures.

To conclude, carbon oxides formation was thoroughly investigated in the case of oxidative coupling of methane. However, current knowledge of the mechanism involved in generating carbon oxides is very limited. In fact, the origin of carbon oxides might be described either heterogeneously or homogeneously. In addition, in the case of propane, CO_x might form directly from (i) propane, and (ii) any other intermediates such as alkenes or alkyl radicals, generated during propane activation [40,41]. In this respect, Lin et al. proposed that an important source of carbon oxides is the homogeneous oxidation of methyl radicals with gas phase oxygen through the formation of methyl peroxy radicals ($CH_3O_2^{\bullet}$) [42]. In fact, their subsequent reactions in the gas phase produce carbon oxides. On the other hand, Nelson et al. proposed a mechanism involving surface reactions of $CH_3O_2^{\bullet}$ species to CO_x [43]. Tong and Lunsford investigated yet another way for the formation of carbon dioxide, during the catalytic coupling of methane, which involves the heterogeneous oxidation of methyl radicals by collision methyl radicals with the metal oxide surfaces [44]. Furthermore, Peil et al. also investigated the reaction of CH_4 with adsorbed atomic oxygen to yield adsorbed CO and CO_2 subsequently released into the gas phase [45]. In our experiments, during pulses of propane, evolution of CO and CO_2 in the gas phase was not observed. Therefore, we conclude that CO and CO_2 formation during the oxidative conversion of propane over Li/MgO catalysts is not caused by active lattice oxygen. Carbon oxides might be formed mainly in the gas phase (when propane and oxygen are simultaneously present). However, the role of adsorbed oxygen molecules on the catalyst surface cannot be ruled out and it is not here investigated.

5. Conclusions

Our findings demonstrate that the number of surface $[O^-]$ active sites in Li-promoted MgO catalysts can be independently estimated by studying, respectively, the interaction of H_2 and O_2, and the sorption/desorption cycles of CO_2. The results obtained from the two methods are in good agreement. We conclude that the surface areas of Li-promoted MgO catalysts can be tuned using different preparation methods maintaining the same number of $[Li^+O^-]$ active sites per m^2 of material.

Propane activation occurs *via* abstraction of hydrogen on the $[Li^+O^-]$ centers forming hydroxyl groups. Our investigations of active sites regeneration suggested that at 550 °C water formation during oxidative dehydrogenation proceeds without removal of lattice oxygen. Further, CO_x formation is not caused by participation of lattice oxygen. In contrast, at higher temperatures (i.e., 700 °C) evolution of water seems to involve lattice oxygen as in redox routes involving anion vacancies.

Acknowledgements

The authors gratefully would like to thank B. Geerdink for technical support and L. Vrielink for XRF and nitrogen sorption measurements. A special thanks to CW/NWO, The Netherlands, for financial assistance. This work was performed under the auspices of the Dutch Institute for Research in Catalysis (NIOK).

References

[1] R.K. Grasselli, D.L. Stern, J.G. Tsikoyiannis, Appl. Catal. A: Gen. 189 (1999) 1.
[2] F. Nierlich, Hydrocarbon Process. 71 (1992) 45.
[3] Petrochemistry Activity Review, http://www.cefic.org/.
[4] M.M. Bhasin, J.H. McCain, B.V. Vora, T. Imai, P.R. Pujado, Appl. Catal. A: Gen. 221 (2001) 397.
[5] E.A. Mamedov, V. Cortes Corberan, Appl. Catal. A: Gen. 127 (1995) 1.
[6] F. Cavani, F. Trifiro, Catal. Today 36 (1997) 431.
[7] H.H. Kung, Adv. Catal. 40 (1994) 1.
[8] L. Leveles, K. Seshan, J.A. Lercher, L. Lefferts, J. Catal. 218 (2003) 296.
[9] L. Leveles, K. Seshan, J.A. Lercher, L. Lefferts, J. Catal. 218 (2003) 307.
[10] F. Cavani, F. Trifiró, Catal. Today 24 (1995) 307.
[11] J.X. Wang, J.H. Lunsford, J. Phys. Chem. 90 (1986) 5883.
[12] J.H. Lunsford, Langmuir 5 (1) (1989) 12.
[13] J.H. Lunsford, Adv. Catal. 35 (1987) 139.
[14] M.C. Wu, C.M. Troung, K. Coulter, D.W. Goodman, J. Vasc. Sci. Technol. A 11 (4) (1993) 2174.
[15] I. Balint, K.-I. Aika, J. Chem. Soc. Faraday Trans. 91 (12) (1995) 1805.
[16] K.D. Campbell, J.H. Lunsford, J. Phys. Chem. 92 (1988) 5792.
[17] D.J. Driscoll, J.H. Lunsford, J. Phys. Chem. 89 (1985) 4415.
[18] T. Ito, J.X. Wang, C.H. Lin, J.H. Lunsford, J. Am. Chem. Soc. 107 (1985) 5062.
[19] D.J. Driscoll, W. Martir, J.X. Wang, J.H. Lunsford, J. Am. Chem. Soc. 107 (1985) 58.
[20] C. Trionfetti, I.V. Babich, K. Seshan, L. Lefferts, Langmuir 24 (15) (2008) 8220–8228. , doi:10.1021/la8006316.
[21] C. Trionfetti, I.V. Babich, K. Seshan, L. Lefferts, Appl. Catal. A: Gen. 310 (2006) 105.
[22] C. Trionfetti, I.V. Babich, K. Seshan, L. Lefferts, Top. Catal. 39 (3–4) (2006) 191.
[23] http://webbook.nist.gov/chemistry/.
[24] R. Burch, E.M. Crabb, Appl. Catal. A: Gen. 100 (1993) 111.
[25] V.P. Vislovskiy, T.E. Suleimanov, M.Y. Sinev, Y.P. Tulenin, L.Y. Margolis, V. Cortes Corberan, Catal. Today 61 (2000) 287.
[26] M.A. Johnson, E. Stefanovich, T.N. Truong, J. Phys. Chem. 101 (1997) 3196.
[27] C. Shi, M.P. Rosynek, J.H. Lunsford, J. Phys. Chem. 98 (1994) 8371.
[28] K.-I. Aika, J.H. Lunsford, J. Phys. Chem. 81 (14) (1977) 1393.
[29] S.C. Bhumkar, L.L. Lobban, Ind. Eng. Chem. Res. 31 (1992) 1856.
[30] D. Wang, M. Xu, C. Shi, J.H. Lunsford, Catal. Lett. 18 (1993) 323.
[31] S.J. Korf, J.A. Roos, N.A. de Bruijn, J.G. van Ommen, J.R.H. Ross, J. Chem. Soc. Chem. Commun. (1987) 1433.
[32] R.C. Weast, Handbook of Chemistry and Physics, 64th ed., CRC Press Inc., Florida, 1984, pp. B106 and B108.
[33] A.L. Shluger, R.W. Grimes, C.R.A. Catlow, N. Itoh, J. Phys. Condens. Matter 3 (1991) 8027.
[34] A.M. Ferrari, G. Pacchioni, J. Phys. Chem. 99 (1995) 17010.
[35] M.Y. Sinev, V.Y. Bychkov, V.N. Korchak, O.V. Krylov, Catal. Today 6 (1990) 543.
[36] M.Y. Sinev, Catal. Today 24 (1995) 389.
[37] M.Y. Sinev, V.Y. Bychkov, Kinet. Katal. 34 (1993) 309.
[38] M. Machli, C. Boudouris, S. Gaab, J. Find, A.A. Lemonidou, J.A. Lercher, Catal. Today 112 (2006) 53.
[39] M.Y. Sinev, Z.T. Fattakhova, Y.P. Tulenin, P.S. Stennikov, V.P. Vislovskii, Catal. Today 81 (2003) 107.
[40] K. Otsuka, K. Jinno, A. Morikawa, J. Catal. 100 (1986) 353.
[41] J.A. Roos, S.J. Korf, R.H.J. Veehof, J.G. van Ommen, J.R.H. Ross, Appl. Catal. 52 (1989) 147.
[42] C.H. Lin, T. Ito, J.X. Wang, J.H. Lunsford, J. Catal. 111 (1988) 302.
[43] P.F. Nelson, C.A. Lukey, N.W. Cant, J. Catal. 120 (1989) 216.
[44] Y. Tong, J.H. Lunsford, J. Am. Chem. Soc. 113 (1991) 4741.
[45] K.P. Peil, J.G. Goodwin, G. Marcelin, J. Phys. Chem. 93 (1989) 5977.